The impact of attenuated phase shift mask topography on hyper-NA lithography

Chris A. Mack, Mark D. Smith, Trey Graves
KLA-Tencor, FINLE Division
8834 N. Capital of Texas Highway, Suite 301, Austin, TX 78759 USA
e-mail: mark.d.smith@kla-tencor.com

ABSTRACT

Thin mask approximations and Kirchhoff boundary conditions for imaging calculations are justified when patterns on masks are large compared to the imaging wavelength and the thickness of absorber films were relatively small compared with the wavelength. For the future technology nodes, these assumptions will not be sufficiently accurate for simulation of attenuated phase shift masks. At very high numerical apertures and extreme off-axis illumination angles, changes in the optical path length and shadowing by the mask topography can lead to phase and amplitude deviations between the thin mask approximation and the more rigorous, full Maxwell equations approach. We have found a systematic, non-constant transmission and phase variation through pitch for low k1 imaging that is not found with the thin-mask approach. In this paper, the major impacts of attenuated phase shift mask topography in the presence of extreme off-axis illumination with numerical apertures greater than one is investigated and the contribution of mask topography to CD errors on the wafer is explored. Consideration of this new mask component to CD error budgets is needed when debating the advantages and disadvantages in a reticle magnification change.

Keywords: Lithography Modeling, mask topography, PROLITH

1. Introduction

Many lithography simulation softwares, such as OPC decoration engines, employ the thin-mask approximation for imaging calculations. While it is well known that a more rigorous approach is often needed for alternating phase-shift reticles, it is not clear how mask topography will affect attenuated phase shift masks (also called embedded phase shift masks, EPSM) in the hyper-NA regime. In the past, patterns on masks were large compared to the imaging wavelength and the thickness of attenuated PSM films were relatively small compared with the wavelength. For the future technology nodes, this will not be true. At very high numerical apertures and extreme off-axis illumination angles, changes in the optical path length and shadowing by the mask topography can lead to phase and amplitude deviations between the thin mask approximation and the more rigorous, full Maxwell equations approach.

High NA mask topography effects come from two sources. As the NA is increased, smaller feature sizes on the mask are enabled by the improved resolution. These smaller features will exhibit more topography effects as the primary features approach a wavelength of light on a 4X reticle. The second source has to do with the larger illumination angles that come with the larger NA, especially when extreme off-axis illumination is used. We have found a systematic, non-constant variation in the phase and amplitudes of the diffraction orders through pitch for low k1 imaging that can not be found with the thin-mask approach. While previous work approximated some of these errors as a mask bias [1], this work takes a more in depth look and attributes the errors to effective phase and transmission errors. By using rigorous mask simulations,

25th Annual BACUS Symposium on Photomask Technology, edited by J. Tracy Weed, Patrick M. Martin,
Proc. of SPIE Vol. 5992, 59920Z, (2005) · 0277-786X/05/$15 · doi: 10.1117/12.632510

the impact of smaller features and higher angles of illumination on the magnitude and phase of the resulting diffraction orders is calculated. The lithographic impact of mask topography is assessed by relating changes in the diffraction orders to effective phase and transmission errors of the EPSM, which in turn are related to focus shifts, effective mask bias, and effective dose errors.

2. Thin Film Theory

Actual attenuated phase shift masks are made of two or three layers coated on a fused silica substrate. However, to start we will examine the simpler case of a single attenuating film. Multiple film stacks for the attenuator will be discussed at the end of this paper. The phase and amplitude transmittance of a thin absorbing film between two dielectrics (quartz and air, in this case) is a standard problem worked out in the classic optics textbook by Born and Wolf [2]. The results, however, are more complex than one might imagine. Difficulties arise because the interpretation of Snell's law becomes less than straightforward when one or both of the materials are absorbing (for example, light traveling from quartz into the absorber). For such a case, the refractive index is complex, leading to a Snell's law equation with a complex angle of refraction. How is a complex angle of transmittance to be interpreted? It means that the surfaces of constant phase are not parallel to the surfaces of constant amplitude (the light is said to be an inhomogeneous wave).

In any case, careful attention to the mathematic details provides the correct solution, for example equations (24) and (25) in section 13.4 of Born and Wolf [2]. The intensity and phase transmittance of the film as a function of angle for *s*-polarization is shown in Figure 1 using the Born and Wolf solution. Here the film is assumed to have an index of 2.343 + *i*0.5536 and a thickness of 73.5nm, and a quartz blank of index 1.5. The sine of the maximum possible angle of light striking the mask is the numerical aperture of the scanner divided by the reduction ratio. Thus, for a 4X mask at NA = 0.8, the maximum angle possible for any illuminator is 11.5º. For NA = 1.0, the maximum angle is 14.5º. For an immersion NA of 1.2, the maximum possible angle increases to 17.5º. The angle exceeds 20º for an NA of 1.4.

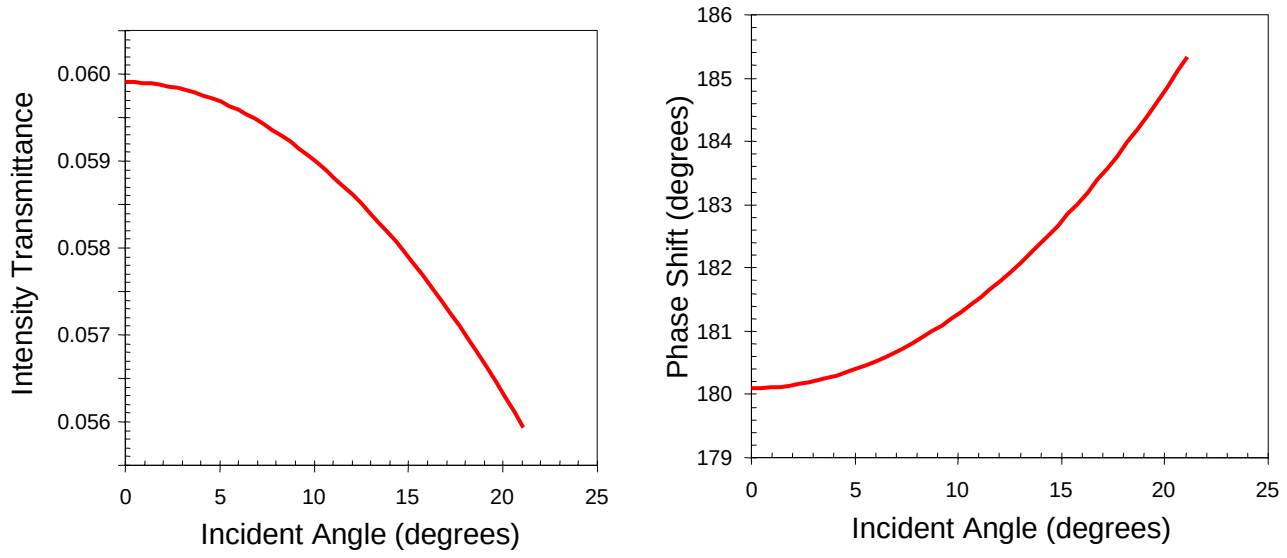

Figure 1. The transmittance of an absorbing film (***n*** = 2.343 + *i*0.5536 and a thickness of 73.5nm) on quartz (*n* = 1.5), relative to the transmittance of the quartz blank, for *s*-polarized illumination.

Since the absorber for the nominal 6% attenuator is fairly absorbing, the exact transmission expressions from Born and Wolf can be simplified. For this high absorption case, the phase transmittance is about equal to the "geometric" phase shift (due to the optical path length) plus the phase changes that occur at the quartz/absorber boundary and the absorber/air boundary. For the optical conditions listed above, the quartz/absorber boundary exhibits a -8.2º phase change that varies by only 0.05º over the angular range shown in Figure 1. The absorber/air boundary shows a +3.9º phase change that varies by 0.15º over the same angular range. Thus, to a good approximation, the combined phase change at the two interfaces of the absorber is -4.3º, going to -4.5º at a 20º incident angle. It is clear that phase variations of the interface transmission coefficients with angle are not a significant part of the total phase variation seen in Figure 1.

Taking into account the -4.3º phase change at the interfaces, the needed geometric phase shift for *s*-polarization is about 184.3º. The geometric phase shift is given by

$$\Delta\phi = 2\pi(n_{film}\cos(\theta_{film}) - \cos(\theta_{air}))D/\lambda \qquad (1)$$

where D is the thickness of the absorber, n_{film} is the real part of the absorber index of refraction, and θ_{film} is the angle of the light in the absorber when assuming no absorption in the film (that is, as calculated from Snell's law using only the real part of the film refractive index). Equation (1) is accurate to about 0.3º for these optical conditions, and this error varies by only 0.07º over the 20º incident angle range. It is this geometric phase effect that gives rise to almost all of the 5º or so phase error that results from illuminating the attenuated PSM at a 20º incident angle.

In conclusion, hyper-NA lithography tools will greatly increase the incident angles that illuminate photomasks, going from the 10-12º maximum angles that masks experience today to upwards of 20º for future immersion systems. As a result, our thin film analysis shows that attenuated PSM phase errors of up to 5º and intensity transmission errors of about 0.4% can be expected. As will be shown below, however, these errors are a very small part of the mask topography effects that are expected for hyper-NA lithography.

3. Effect of Attenuated PSM Phase Errors

How does a small phase error affect the lithographic performance of an attenuated PSM? Consider a pattern of lines and spaces with spacewidth w_s and linewidth w_l. The electric field amplitude and phase transmittance of the line will be T and φ, respectively. (Note that for a 6% EPSM, $T \approx 0.245$.) Because the mask is a repeating pattern of lines and spaces, the resulting diffraction pattern will be discrete diffraction orders. For high resolution patterns only the zero and first diffracted orders will pass through the lens and be used to generate the aerial image. Defining a coordinate system with x=0 at the center of the space and letting $p = w_s + w_l$ = the pitch, the amplitude of the zero and first diffraction orders will be given by

$$a_0 = \frac{w_s}{p} + \frac{w_l}{p}Te^{i\varphi}$$

$$a_1 = a_{-1} = \frac{\sin(\pi w_s/p)}{\pi} - \frac{\sin(\pi w_l/p)}{\pi}Te^{i\varphi} \qquad (2)$$

For equal lines and spaces,

$$a_0 = \frac{1}{2}\left(1+Te^{i\varphi}\right)$$

$$a_1 = a_{-1} = \frac{1}{\pi}\left(1-Te^{i\varphi}\right) \tag{3}$$

For an ideal attenuated PSM $\varphi = \pi$ (180º), and equation (3) becomes

$$a_0 = \frac{1}{2}(1-T)$$

$$a_1 = a_{-1} = \frac{1}{\pi}(1+T) \tag{4}$$

Thus, equation (4) shows us that the effect of the attenuated PSM as compared to a chrome on glass mask is to reduce the magnitude of the zero order and increase the magnitude of the first order (which results in a higher contrast image). The standard 6% EPSM produces zero and first orders of about equal amplitude.

For a mask with phase error, we can let $\varphi = \pi + \Delta\varphi$. Using this value in equation (3), and assuming that the phase error is small,

$$a_0 = \frac{1}{2}\left(1-Te^{i\Delta\varphi}\right) = \frac{1}{2}(1-T\cos(\Delta\varphi)) - i\frac{1}{2}T\sin(\Delta\varphi) \approx \frac{1}{2}\left(1-T+\frac{T\Delta\varphi^2}{2}\right) - i\frac{1}{2}T\Delta\varphi$$

$$a_1 = a_{-1} = \frac{1}{\pi}\left(1+Te^{i\Delta\varphi}\right) \approx \frac{1}{\pi}\left(1+T-\frac{T\Delta\varphi^2}{2}\right) + i\frac{1}{\pi}T\Delta\varphi \tag{5}$$

Calculating the magnitude and the phase of each of each diffraction order,

$$|a_0| \approx |a_0|_{ideal} + \frac{\Delta\varphi^2}{4}\left(\frac{T}{1-T}\right)$$
$$\angle a_0 \approx -\Delta\varphi\left(\frac{T}{1-T}\right) \tag{6}$$

$$|a_1| \approx |a_1|_{ideal} - \frac{\Delta\varphi^2}{2\pi}\left(\frac{T}{1+T}\right)$$
$$\angle a_1 \approx \Delta\varphi\left(\frac{T}{1+T}\right) \tag{7}$$

Let's investigate the impact of the changes in the magnitude and phase of each diffracted order separately. As shown in equations (6) and (7), the magnitudes of the orders vary as the phase error squared (and so should be quite small for small errors). As an example, for a 6% EPSM with a 10º phase error the zero and

first orders change by only +0.7% and -0.2% respectively. The resulting impact on the aerial image is quite small, less than 0.2% intensity difference in most cases.

The phase of the diffraction orders, on the other hand, vary directly as the EPSM phase error. In fact, the phase difference between the zero and first orders, which ideally would be zero, becomes in the presence of EPSM phase error

$$\angle a_1 - \angle a_0 \approx \frac{2\Delta\varphi T}{1+T^2} \tag{8}$$

Evaluating equation (8) for a nominal 6% EPSM mask, the difference in diffraction order angles would be about $0.46\Delta\varphi$.

What is the impact of such a change in the phase difference between the diffraction orders? Focus also causes a phase difference between the zero and first orders. For the simple case of coherent (normally incident) illumination, a defocus of δ causes a phase difference of

$$\angle a_1 - \angle a_0 \approx \frac{\pi \delta \lambda}{p^2} \tag{9}$$

Thus, for this three beam imaging case the effect of the EPSM phase error will be to shift best focus by an amount given by

$$\delta_{shift} \approx \frac{2p^2\Delta\varphi T}{\pi\lambda(1+T^2)} \tag{10}$$

Fortunately, a quick look at the magnitude of this focus shift shows that it is reasonably small. For a 6% EPSM at 193nm wavelength, focus will shift between 0.5 and 2nm per degree of EPSM phase error, with the smallest shifts occurring for the smallest features. Remembering that equation (10) was derived under the simple assumption of coherent illumination, full image simulations show that the use of partial coherence can double or triple the focus shift compared to the coherent case. Off-axis illumination, however, tends to lower this effect since this illumination is specifically intended to give 2-beam imaging. A phase difference between diffraction orders for 2-beam imaging will produce an image tilt, resulting in a placement error. However, since the right and left poles of a quadrupole illuminator, for example, will create shifts in opposite directions, the effect will be a degradation of the image, but no net image shift. Figure 2 illustrates this focus-shift effect for coherent illumination showing also that, unlike alternating PSM, there is no pattern placement change through focus in the presence of an EPSM phase error.

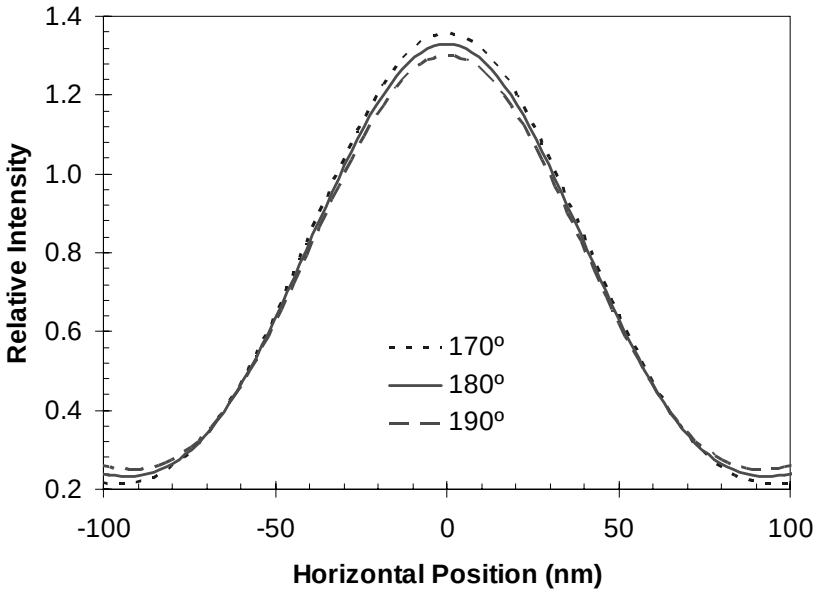

Figure 2. A small phase error in an EPSM mask changes the aerial image in the same way as a small shift in focus. Here, ±10º phase error moves the image closer and farther away from best focus for this out of focus image (wavelength = 193nm, NA = 0.93, 130nm lines/space pattern, coherent illumination, 50nm defocus). For this case, a 10º phase error shifts best focus by about 9nm.

4. Effect of Attenuated PSM Transmission Errors

A similar analysis to that above can be used to assess the impact of small transmission errors on the lithographic performance of an attenuated PSM. For equal lines and spaces, a small electric field transmission error of ΔT will change the zero and first diffraction orders to be

$$a_0 = a_{0-ideal} - \frac{\Delta T}{2}$$

$$a_1 = a_{1-ideal} + \Delta T \tag{11}$$

Thus, an increase in the EPSM transmission will decrease the zero order while increasing the first orders by twice that amount. The most useful way to represent changes in both zero and first order magnitudes is by looking at their ratio. For small transmission errors,

$$\frac{a_0}{a_1} \approx \frac{a_{0-ideal}}{a_{1-ideal}} - \frac{\pi \Delta T}{2(1+T)}\left[\pi\left(\frac{1-T}{1+T}\right)+1\right] \tag{12}$$

Evaluating equation (12) for a nominal 6% EPSM mask, the diffraction order amplitude ratio would decrease with transmission error by about 3.7ΔT.

The lithographic impact of a small intensity transmission error will be similar to a bias on the mask. If a small bias Δw is applied to the equal lines and spaces, (a positive value increasing the line width and decreasing the space width), the impact on the first order will be negligible, but the zero order will become

$$a_0 = a_{0-ideal} - \frac{\Delta w(1+T)}{p} \tag{13}$$

One can approximate a transmission error as a dose error (which increases the magnitude of both the zero and first orders) plus a bias (which decreases the zero order). The effective fractional dose error is

$$\frac{\Delta dose}{dose} \approx \frac{2\pi \Delta T}{1+T} \tag{14}$$

and the effective mask bias is

$$\frac{\Delta w}{w} \approx \frac{\Delta T}{(1+T)}\left[\pi\left(\frac{1-T}{1+T}\right)+1\right] \tag{15}$$

Consider the standard 6% EPSM (T = 0.245). Equations (14) and (15) become (again, for equal lines and spaces)

$$\frac{\Delta dose}{dose} \approx 5\Delta T\,, \qquad \frac{\Delta w}{w} \approx 1.3\Delta T \tag{16}$$

If the intensity transmittance decreases 0.5% (the amplitude transmittance would decrease by 1%), it would be roughly equivalent to a 5% dose decrease and a -1.3% mask bias. However, to some extent these errors work against each other, partially canceling out.

5. Rigorous Mask Topography Simulations

The above expressions for the impact of small phase and transmission errors on the zero and first diffraction orders for a pattern of equal lines and spaces can now be conveniently used to characterize mask topography effects for a 6% EPSM mask. Rigorous Maxwell's equations solutions at the mask performed using PROLITH can provide calculations of the amplitudes and phases of the diffraction orders. But it is difficult to turn this data into an intuition about the lithographic consequences. Our approach here will be to relate changes in the amplitude ratio and phase difference between the zero and first diffraction orders to effective phase and transmission errors of the EPSM:

$$\angle a_1 - \angle a_0 \approx 0.46\Delta\varphi\,, \qquad \left|\frac{a_0}{a_1}\right| \approx \frac{a_{0-ideal}}{a_{1-ideal}} - 3.6\Delta T \tag{17}$$

PROLITH v9.1 was used to simulate a simplified one layer EPSM film stack using the EMF1 algorithm (a rigorous coupled wave analysis method) at speed factor 1. The ideal film stack from above was used (an index of 2.343 + i0.5536 and a thickness of 73.5nm, and a quartz blank of index 1.5). A y-oriented equal line/space pattern was simulated through pitch, with results shown in Figure 3. By using the approximate expressions (17), effective phase and intensity transmittance errors were calculated as shown in Figure 4.

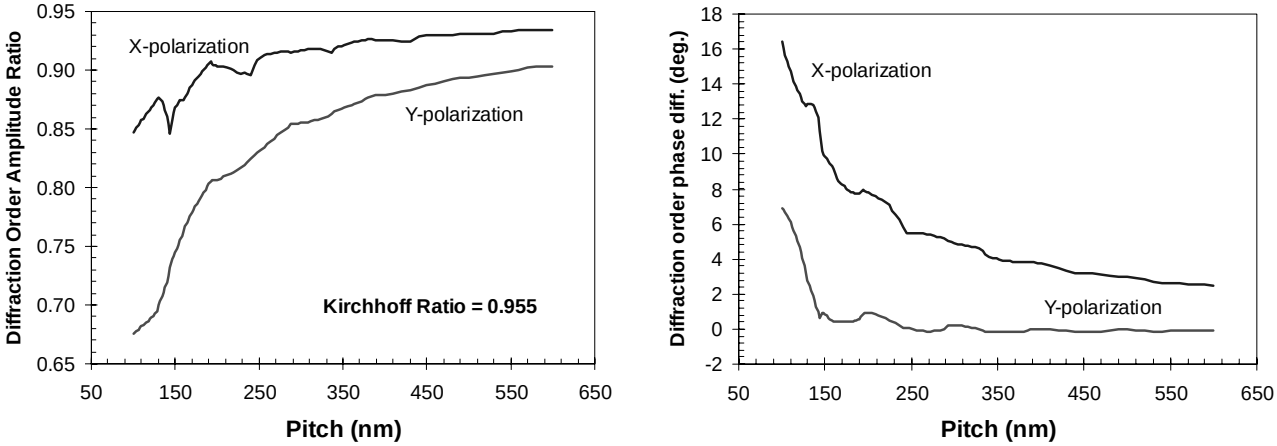

Figure 3. Using PROLITH EMF simulations, the impact of pitch (for equal lines and spaces) on the zero and first diffraction orders. Normal incidence of illumination was used.

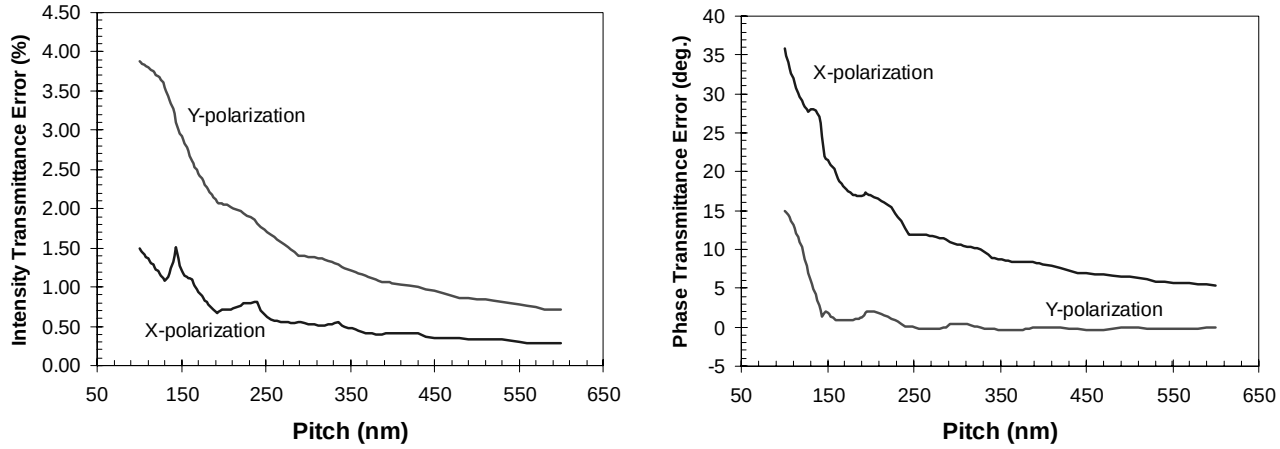

Figure 4. Using the approximate expressions (17), translation of the EMF simulation data of Figure 3 into effective EPSM phase and transmittance errors.

Several interesting and important trends can be seen in Figures 3 and 4. As expected, smaller features show the greatest deviation from ideal Kirchhoff thin-mask behavior. For all cases, behavior approaches the ideal behavior as the pitch gets bigger, but the rate of approach is polarization dependent. For x-polarization on these y-oriented lines and spaces, the effective transmission error of the mask is smallest, and more quickly falls to low values. By about a pitch of about 250 to 300nm, the x-polarization transmission error has nearly leveled off. For y-polarization, the intensity transmission error is still going down at a pitch of 600nm. For effective phase transmission errors, the opposite trend is observed. The y-polarization case has phase errors of 15º at the smallest pitch of 100nm, but quickly drops to zero error at a 140nm pitch. For the x-polarization case, the effective EPSM phase errors are much larger, and don't approach zero until the pitch is much larger than 600nm. It is important to remember that the y-polarization

is the "good" polarization for the y-oriented features. For polarization controlled lithography tools, it will be the y-polarization that is used.

Figures 5 – 7 take one pitch, 130nm, and explore the impact of the angle of incidence of the mask illumination. There are two types of angles, radial and azimuthal. The radial angle is labeled x-angle in these figures since the angle spreads along the x-axis. It is this angle that experiences an asymmetric shadowing due to the thickness of the absorber. As a result, the $+1^{st}$ order is not the same as the -1^{st} order in magnitude or phase. However, since the high incident angles occur during off-axis illumination, in general only one of these orders will be used anyway. Thus, Figure 5 references the zero order to the $+1^{st}$ order, while Figure 6 references the zero order to the -1^{st} order. Figure 7 sets the azimuthal angle at 90º so that the angle of incidence is spread along the y-axis. For this angle, the right and left sides of the feature edges are shadowed symmetrically so that both first orders as the same.

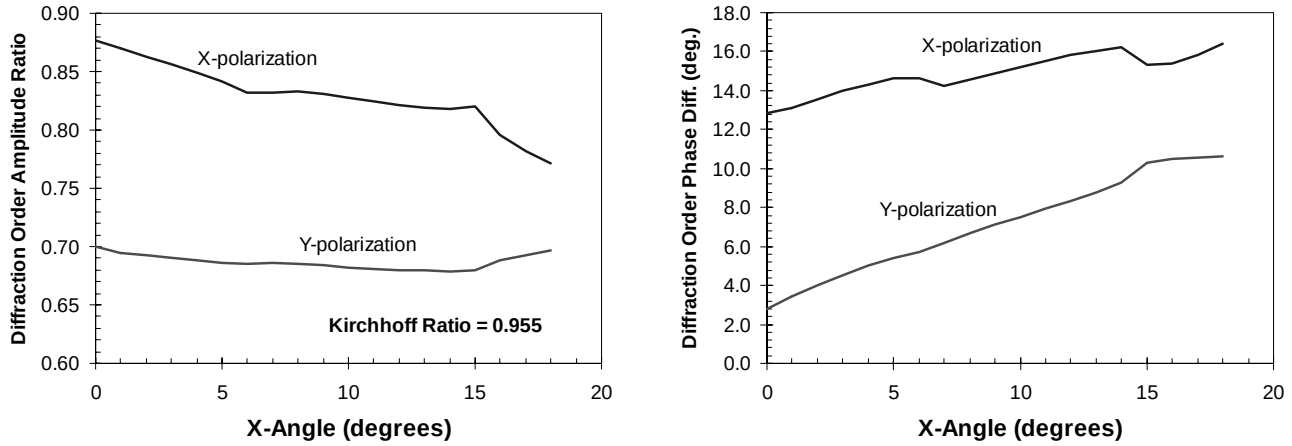

Figure 5. Using PROLITH EMF simulations, the impact incident angle spread along the x-axis (for 65nm equal lines and spaces) on the zero and +first diffraction orders.

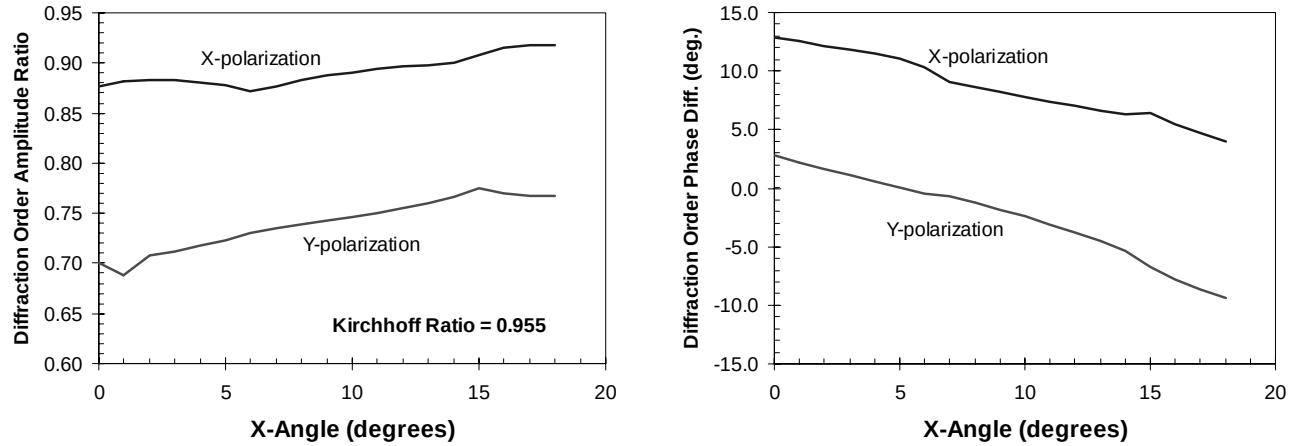

Figure 6. Using PROLITH EMF simulations, the impact incident angle spread along the x-axis (for 65nm equal lines and spaces) on the zero and -first diffraction orders.

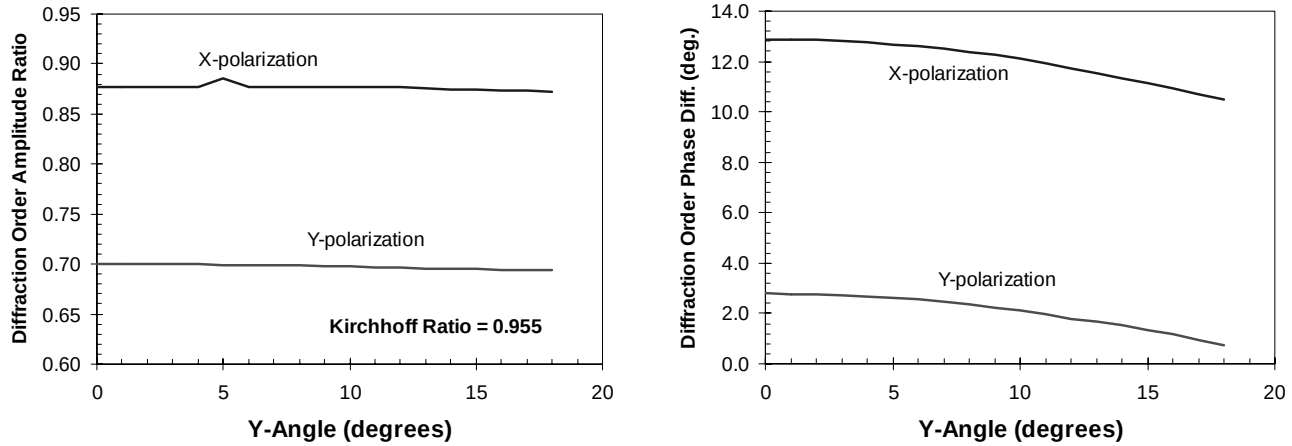

Figure 7. Using PROLITH EMF simulations, the impact incident angle spread along the y-axis (for 65nm equal lines and spaces) on the zero and first diffraction orders.

One can clearly see by comparing Figure 7 to Figures 5 and 6 that the asymmetric shadowing of the x-angles is clearly more significant than the impact of the y-angles. As the thin film calculations in section 2 showed, the geometric phase and transmission errors are quite small out to 20º incident angle. Interestingly, though, the variations predicted by combining the data from Figure 1 with the simple expressions in equation (17) predict and increase in diffraction order phase difference, rather than the decrease shown in Figure 7. Thus, even for this case the mask topography interactions with the light has a bigger impact than the simple geometric optical path length effect.

6. Conclusions

The impact of mask topography on the imaging behavior of alternating phase shift masks is well known and has been the subject of numerous studies. The sensitivity of attenuated PSM (also called embedded or EPSM) to mask topography effects has always been assumed to be small, but little quantitative work has been done to verify this assumption. In this study, electromagnetic field simulations were carried out to study the mask topography effects of a simplified 6% attenuated PSM. A unique approach was developed for this purpose. Using analytic expressions for the diffraction patterns of EPSM line/space mask patterns under the Kirchhoff assumption, small changes in the phase and amplitude of the diffraction orders were related to small phase and amplitude transmission errors of the EPSM material. Next, rigorous EMF simulations were performed on line/space patterns through pitch and for a range of incident angles to calculate the complex zero and first diffraction orders. Using the small error analytic Kirchhoff expressions for these diffraction orders, effective phase and transmission errors were assigned to the effects of mask topography. Thus, the important but non-intuitive output of an EMF calculation – diffraction order phase and amplitudes – could be related to more intuitive effects – phase and amplitude transmission errors in the EPSM material.

Using the above approach, interesting mask topography effects were elucidated. For the very small pitches that will soon be possible with 193nm immersion lithography, mask topography effects for a 6%

EPSM are significant. The effects are extremely polarization dependent, feature size dependent, and incident angle dependent.

The simulation and analysis approach given here seems quite valuable, but more work should be done to fully evaluate EPSM mask topography effects. Full characterization of the lithographic consequences is needed, as well as the examination of more isolated patterns.

7. References

1. M. D. Smith, J. D. Byers, and C. A. Mack "The impact of mask topography on binary reticles at the 65nm node," *23rd Annual BACUS Symposium on Photomask Technology*, *Proc*., SPIE Vol. 5567 (2004).

2. M. Born and E. Wolf, Principles of Optics, Sixth Edition, Pergamon Press (Oxford: 1980), p. 631.